Journal of Applied Mechanics and Technical Physics, Vol. 35, No 6, 1994

MODEL OF THE DEFORMATION OF A LIQUID DROPLET IN A GAS FLOW

D. A. Detkovskii and S. M. Frolov

UDC 532.529

1. INTRODUCTION

The deformation and breakup of liquid droplets play a key role in many applied problems involving multiphase flows, for example, in engine combustion [1] and explosion safety [2]. This situation fosters a continued interest in the subject and the ongoing publication of new experimental [3-6] and theoretical [7-9] papers. Noteworthy among earlier experimental studies are [10-19], in which the basic laws of the phenomenon have been investigated. Detailed surveys of earlier research in the area can be found in [4, 20].

Two approaches have surfaced in theoretical papers: 1) the analysis of the complex stressed state of a droplet on the basis of multidimensional equations of motion [8, 9, 21]; 2) the construction of simplified phenomenological models [22-24]. The successes of the first approach stem primarily from the advancement of computer engineering, but there have also been auspicious attempts at the purely analytical approach [21]. Simplified models of the deformation and breakup of droplets are better justified in the investigation of complex, chemically reacting, multiphase flows [25, 26].

Certain obvious requirements must be met by any simplified model of droplet deformation, namely it should:

— give acceptable results on the dynamics and characteristic time of deformation of the droplet to the critical stage, i.e., the time at which deformation becomes irreversible;

— give correct values of the minimum (critical) Weber number necessary for the droplet to attain irreversible deformation;

— correctly mirror the dependence of the characteristic deformation time and the critical Weber number on the governing parameters.

A good criterion of the validity of a model is its conformity with experimental observations.

The model of [22], which is used in [25, 26], does not meet the stated requirements. The model of [23], which is based on the equation for the deformation of a liquid ellipsoid in a gas flow, ignores the viscous properties of the liquid and the gas. A simplified droplet deformation model based on the "preferred direction of deformation" (PDD) approximation has been proposed by Davidson [24]. The PDD approximation is geared to the uniaxial stressed state of a particle of a viscous, incompressible liquid under the influence of forces created by aerodynamic pressure, surface tension, and gravity. The model is based on the Stokes friction law, which relates the linear strain rate of a particle to the normal stress. The results of calculations according to the model give a qualitative correct picture of the droplet deformation dynamics and the dependence of the critical Weber number on the governing parameters. Quantitatively, however, Davidson's model [24] yields greatly underestimated values of the characteristic deformation time and critical Weber numbers.

A new droplet deformation model based on the PDD approximation is proposed below. The main departure from Davidson's model [24] is an attempt to include internal viscous flows in the droplet as it undergoes deformation. The model is used to calculate the deformation dynamics and critical Weber numbers when the droplet is loaded in an airborne shock wave.

2. STATEMENT OF THE PROBLEM

Suppose that the initial droplet is in the shape of a sphere of radius R. The direction of motion of the droplet (x axis) coincides with the direction of the unrestricted gas flow. We introduce the following simplifying assumptions:

Moscow. Translated from Prikladnaya Mekhanika i Tekhnicheskaya Fizika, No. 6, pp. 105-114, November-December, 1994. Original article submitted January 19, 1994.

0021-8944/94/3506-0911$12.50

1) The deformation of the droplet is analyzed in the PDD approximation.

2) The droplet is deformed quasistatically, i.e., the deformed state at each instant is determined from the condition of equilibrium of all active forces.

3) The liquid is incompressible, the mass of the droplet is invariant during deformation, and the additional mass of the droplet is negligible.

4) The deformed droplet is in the shape of an ellipsoid of revolution, prolate in the direction transverse to the flow, and the ellipsoid is formed by the rotation of an ellipse of semiminor axis a and semimajor axis b about the minor axis.

5) The influence of the force of gravity is negligible.

6) The deformation process become irreversible when a certain critical strain is attained, at which point $a = a_*$ and $b = b_*$.

We place the origin at the center of symmetry of the droplet. In the PDD approximation we write the equation for the linear strain of the droplet along the x axis in the form

$$2\mu_l a^{-1}(da/dt) = -K\Delta p, \tag{2.1}$$

where t is the time, μ_l is the dynamic viscosity of the liquid, Δp is the total deforming pressure, and $K < 1$ is a dimensionless coefficient, which takes into account the work done by aerodynamic and surface tension forces in imparting internal motions to the liquid. The coefficient K is what distinguishes Eq. (2.1) from the corresponding equation in [24].

The total deforming pressure is defined as the difference between the total aerodynamic pressure p_d on the surface of the droplet and the normalized Laplacian pressure p_σ in the droplet interior, i.e., $\Delta p = p_d - p_\sigma$. The projection of the total aerodynamic pressure onto the x axis is defined as

$$p_d = \frac{1}{S}\int_S (p - p_0)dS. \tag{2.2}$$

Here p is the x-projection of the pressure-induced force on the surface of the droplet, and p_0 is the static pressure of the gas; the integral is evaluated over the entire surface of the droplet S. Since the liquid is incompressible, the Laplacian pressure induces uniform compression of the droplet. In the PDD approximation, however, two surface tension components can be discerned. The first (positive) component $p_{\sigma+}$ is induced by the curvature of the droplet in the plane parallel to the x axis and tends to flatten the droplet in the direction transverse to the flow. The second (negative) component $p_{\sigma-}$ is induced by the curvature of the droplet in the plane perpendicular to the x axis and tends to restore the droplet to its original shape. In the given approximation the normalized Laplacian pressure has the form

$$p_\sigma = p_{\sigma-} - p_{\sigma+}.$$

For an ellipsoid of revolution we can write [24]

$$p_{\sigma+} = \frac{2\sigma a}{b^2},\ p_{\sigma-} = \frac{\sigma(a^2 + b^2)}{ba^2}. \tag{2.3}$$

The coefficient K is evaluated on the basis of dimensional considerations. It follows from the assumption of quasistatic deformation that K is associated with viscous stresses produced in the steady-state motion of the liquid in the droplet. The functional relation of K to the parameters of the problem can therefore be expressed as

$$K = f(U_l, \mu_l, R, \Delta p_*),$$

where U_l is a characteristic velocity of the liquid, and Δp_* is a characteristic value of the total deforming pressure. The four governing parameters (U_l, μ_l, R, Δp_*) can be consolidated into a single, independent, dimensionless group $U_l\mu_l/R\Delta p_*$. We then have

$$K = \alpha\frac{U_l\mu_l}{R\Delta p_*} \tag{2.4}$$

(α is a numerical coefficient). The velocity U_l is of the same order of magnitude as the droplet deformation rate da/dt, i.e., $U_l(da/dt)^{-1} \sim 1$. This fact provides a means for estimating the order of magnitude of the coefficient α on the basis of (2.1) and (2.4): $\alpha \sim 1$.

To estimate U_l, we invoke the equation of continuity for an incompressible liquid droplet:

$$\frac{1}{r^2}\frac{\partial U_r r^2}{\partial r} + \frac{1}{r\sin\theta}\frac{\partial U_\theta \sin\theta}{\partial \theta} + \frac{1}{r\sin\theta}\frac{\partial U_\varphi}{\partial \varphi} = 0. \tag{2.5}$$

Here U_r, U_θ, and U_φ are the radial and two angular components of the fluid velocity in spherical coordinates. We use Eq. (2.5) for liquid particles on the upstream surface of the droplet and compare the orders of magnitude of the velocity components. A suitable scale of the angular components U_θ and U_φ is the tangential velocity of the droplet surface U_i, which is determined by solving the problem of conjugate boundary layers [27]:

$$U_i = U(\mu\rho/\mu_l\rho_l)^{1/3}$$

(U is the relative velocity of the center of mass of the droplet in the gas flow; quantities without subscripts refer to the parameters of the gas flow).

The radial velocity component varies from $\sim U_l$ to ~ 0 over a distance of the order of R. The angular velocity components vary from ~ 0 (at the stagnation point) to U_i over an angular distance of the order of $\pi/2$. It therefore follows from (2.5) that

$$U_l \sim U_i.$$

Replacing U_l by U_i in (2.3) and setting $\Delta p_* = \rho U^2/2$, we obtain the final expression for the coefficient K

$$K \approx \frac{2\mu_l}{\rho U R}\left(\frac{\mu\rho}{\mu_l\rho_l}\right)^{1/3}. \tag{2.6}$$

In light of Eq. (2.6) we write Eq. (2.1) in the form

$$\frac{da}{dt} = -\frac{1}{2}U\left(\frac{a}{R}\right)\left(\frac{p_d - p_\sigma}{\rho U^2/2}\right)\left(\frac{\mu\rho}{\mu_l\rho_l}\right)^{1/3} \tag{2.7}$$

subject to the initial condition $a = R$ at $t = 0$.

Equation (2.7) contains the relative center-of-mass velocity U of the droplet in the gas flow:

$$U = U_g - U_d$$

(U_g and U_d are the absolute velocities of the gas and the droplet). The equations of motion of the droplet have the form

$$m\frac{dU_d}{dt} = \pi C_x b^2 \frac{\rho U^2}{2}, \tag{2.8}$$

where m is the mass of the droplet, and C_x is the aerodynamic drag coefficient. We assume that U_g is a known function of the time: $U_g = \varphi(t)$. Inasmuch as $dU_d/dt = -dU/dt + d\varphi/dt$ and $m = (4/3)\pi ab^2\rho_l$, we obtain the following in place of (2.8):

$$\frac{dU}{dt} = -\frac{3}{4}\frac{C_x}{a\rho_l}\left(\frac{\rho U^2}{2}\right) + \varphi' \quad (\varphi' = d\varphi/dt) \tag{2.9}$$

subject to the initial condition $U = \varphi(0)$ at $t = 0$.

The drag coefficient of the droplet C_x can be represented by a sum of two terms [28]:

$$C_x = C_{xp} + C_{xi}. \tag{2.10}$$

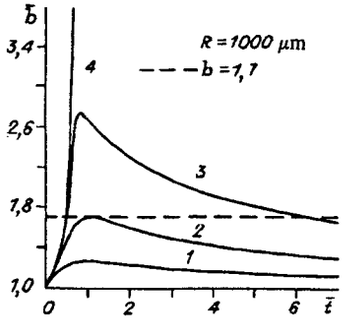

Fig. 1

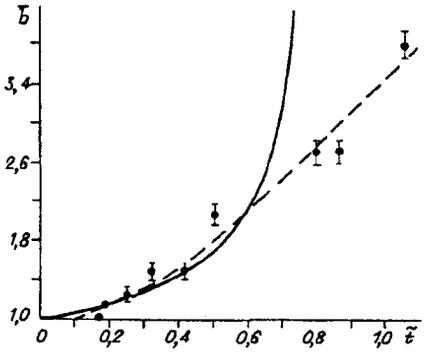

Fig. 2

Here C_{xp} is the pressure drag coefficient, and C_{xi} is the friction drag coefficient. For poorly streamlined bodies such as a deformed droplet at high Reynolds numbers $\mathrm{Re} = \rho UR/\mu$ the approximation $C_{xi} << C_{xp}$ is valid, and Eq. (2.10) reduces to the form $C_x \approx C_{xp}$. In this case C_x is related to the total aerodynamic pressure p_d by the equation

$$C_x = \frac{p_d}{\rho U^2/2} = \overline{p_d} \tag{2.11}$$

($\bar{p}_d$ is the pressure coefficient).

An analysis of experimental data [16] on the drag coefficient of droplets undergoing deformation in compressible gas flows behind shock waves shows that $C_x = 1.8$-3.0 for $\mathrm{Re} > 500$ and does not depend on Re. In other experiments $C_x \approx 2.3$ for $\mathrm{Re} > 10^3$ [3], $C_x \approx 3.0$ for $\mathrm{Re} > 10^4$ [15], and $C_x \approx 1.6$-2.2 for $\mathrm{Re} > 10^3$ [18], where it is noted that C_x depends on how the droplet breaks up. In the present study C_x is assumed to be constant and equal to 2.0, i.e., its average value is adopted.

Consequently, Eqs. (2.7) and (2.9) in conjunction with the initial conditions, relations (2.3), (2.6), and (2.11), and given values of ρ, ρ_l, μ, μ_l, R, and $\varphi(t)$ completely specify the problem of the deformation of a droplet in the PDD approximation.

To transform to dimensionless variables, we introduce the notation

$$t = \bar{t}\left(\frac{\mu_l R}{\sigma}\right),\ U = \sqrt{\frac{\sigma}{\rho R}}\,\mathrm{We}^{1/2},\ \mathrm{We} = \frac{\rho U^2 R}{\sigma},$$

$$a = \bar{a}R,\ b = \bar{b}R,\ \mathrm{La} = \frac{\rho_l \sigma R}{\mu_l^2},\ \bar{\varphi}' = \varphi'\frac{\mu_l R}{\sigma}\sqrt{\frac{\rho R}{\sigma}}.$$

By virtue of assumptions 3 and 4 above, we can write $ab^3 = R^3$. Equations (2.7) and (2.9) then acquire the following form on the basis of (2.3), (2.6), and (2.11):

$$\begin{aligned}\frac{d\bar{a}}{d\bar{t}} &= -\frac{1}{2}\mathrm{We}^{1/2}\mathrm{La}^{-1/2}\left(\frac{\mu}{\mu_l}\right)^{1/3}\left(\frac{\rho_l}{\rho}\right)^{1/6}\left[C_x + \frac{2}{\mathrm{We}}(2\bar{a}^3 - \bar{a}^{3/2} - \bar{a}^{-3/2})\right],\\ \frac{d\mathrm{We}}{d\bar{t}} &= -\frac{3}{4}C_x\frac{\mathrm{We}^{3/2}}{a}\left(\frac{\rho}{\rho_l}\right)^{1/2}\mathrm{La}^{-1/2} + 2\bar{\varphi}'\mathrm{We}^{1/2}\end{aligned} \tag{2.12}$$

subject to the initial conditions $\bar{a} = 1$ and $\mathrm{We} = \mathrm{We}_0$ at $\bar{t} = 0$, where $\mathrm{We}_0 = \rho\varphi^2(0)R/\sigma$. The maximum Weber number We_{0*}, at which the critical deformation stage $\bar{a}_* = \bar{b}_*^{-2}$ is attained, is called the critical Weber number. We use the following procedure to determine $\bar{a}_*$. According to abundant experimental observations of the breakup of droplets in a shock wave, $\mathrm{We}_* \cong 5$ for large-diameter (1-4 mm) droplets of low-viscosity liquids (water, alcohol, and kerosene). The Laplace number $\mathrm{La} = 10^3$-10^5 for droplets of this kind. Since $\rho_l/\rho = 10^2$-10^3, it follows from (2.12) that $d\mathrm{We}/d\bar{t} << 1$ during deformation, i.e., $\mathrm{We} \cong \mathrm{We}_0 = \mathrm{const}$. The reversible deformation of a droplet is characterized by a stage with $d\bar{a}/d\bar{t} = 0$, i.e., according to (2.12),

$$\frac{C_x\mathrm{We}_0}{2} = \bar{a}^{-3/2} + \bar{a}^{3/2} - 2\bar{a}^3. \tag{2.13}$$

TABLE 1

t, msec	$\bar{b}_э$	$\bar{b}$	t, msec	$\bar{b}_э$	$\bar{b}$
	[4]			[6]	
0	1	1	0	1	1
3,61	1,33	1,7	0,2	1,06	1,403
7,23	1,5	1,64	0,4	1,26	1,307
9,17	1,6	1,59	0,65	1,33	1,228
11,12	1,67	1,54	0,7	1,03	1,216
13,90	1,76	1,48	0,8	0,82	1,195
15,29	1,67	1,46	0,9	0,91	1,177
16,12	1,6	1,44			
18,07	1,33	1,41			
23.07	1.26	1.35			

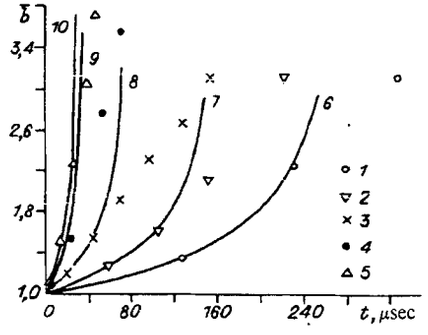

Fig. 3

The critical stage for droplets of low-viscosity liquids sets in when $We_0 = We_{0*} = We_* \approx 5$ and, accordingly, when $\bar{a}_* \approx 0.35$ and $\bar{b}_* \approx 1.7$. We call attention to the difference in the definitions of the critical Weber numbers We_{0*} and We_*: We_{0*} is determined from the initial relative velocity of the gas and the droplet, whereas We_* is determined from the instantaneous relative velocity of the gas and the droplet when the droplet attains the critical deformation stage.

Photographic studies [4] have shown that the maximum deformation of a water droplet ($R = 1300$ μm) before the start of breakup for $We_0 = 6.2$ is $\bar{b} \approx 1.5$-1.62. In experiments [18] with water droplets ($R = 250$ μm) the maximum transverse deformation prior to breakup of a droplet for $We_0 = 6$ was found to be $\bar{b} \approx 2$. The value obtained from (2.13) agrees satisfactorily with these observations. We shall assume below that irreversible deformation of a droplet begins at the indicated values of $\bar{a}_*$ and $\bar{b}_*$ regardless of the properties of the liquid and the impingent gas flow.

We solve the system of equations (2.12) numerically by a fourth-order Runge–Kutta procedure with a variable time step.

3. RESULTS OF THE CALCULATIONS

Since the overwhelming majority of experimental studies of droplet deformation have been conducted with shock waves, we consider the case of sudden loading of a liquid droplet in the flow behind a shock wave with constant parameters. Let M be the Mach number of the shock wave. We calculate the parameters of the gas in Eq. (2.12) according to the equations

$$U = \varphi(0) = \frac{2c_0}{(\gamma - 1)}\left(\mathrm{M} - \frac{1}{\mathrm{M}}\right), \quad \varphi' = 0,$$

$$\rho = \rho_0 \frac{(\gamma + 1)\mathrm{M}^2}{(\gamma - 1)\mathrm{M}^2 + 2}, \quad \mu = 10{,}7 \cdot 10^{-6}(mT)^{1/2} d_m^{-2}, \tag{3.1}$$

$$T = T_0\left[1 + \frac{2(\gamma - 1)}{(\gamma + 1)^2\mathrm{M}^2}(\mathrm{M}^2 - 1)(1 + \gamma\mathrm{M}^2)\right],$$

TABLE 2

Curve No. in Fig. 3	M	We_0	t_d, msec	τ, msec	τ/t_d
6	1,3	$6,7 \cdot 10^3$	430	187	0,43
7	1,5	$2,0 \cdot 10^3$	247	109	0,44
8	2,0	$9,1 \cdot 10^3$	115	52	0,45
9	3,0	$4,1 \cdot 10^4$	54	24	0,45
10	3,5	$6,5 \cdot 10^4$	42	19	0,44

TABLE 3

R, μm	We_0	$\bar{b}$			
		1,1	1,3	1,5	1,7
		$\bar{t}$			
100	5,3	0,12	0,34	0,57	—
150	8,0	0,12	0,31	0,47	0,62
200	11,0	0,12	0,30	0,43	0,54
250	13.0	0.12	0,29	0.41	0,51

where c is the sound velocity, γ is the specific heat ratio, m is the molecular mass, T is the temperature, and d_m is the molecular diameter in angstroms in the model of rigid spheres (see [29]); the subscript 0 refers to the freestream gas parameters. Thus, the set of independent governing parameters for the given droplet loading regime has the form

$$\frac{\rho_0}{\rho_l}, \frac{\mu_0}{\mu_l}, \text{La}, \gamma, \text{M}, \text{We}_0.$$

The following characteristic time is introduced in many studies of droplet breakup processes:

$$t_d = \frac{2R}{U}\sqrt{\frac{\rho_l}{\rho}}.$$

The dimensionless time $\bar{t} = t/t_d$ will be used below to compare the calculated parameters with the experimental data. Figure 1 shows calculated curves of $\bar{b}(t)$ for the deformation of a water droplet (R = 1000 μm) in airborne shock waves of various intensities. Curve 1 (M = 1.02) corresponds to "subcritical" loading of the droplet, since the maximum deformation $\bar{b}_{max} < \bar{b}_*$. After a time $\bar{t} \approx$ 15-20 from the start of loading, the droplet acquires its original spherical shape. Curve 2 (M = 1.033) corresponds to critical deformation $\bar{b}_{max} = \bar{b}_*$, $We_0 = We_{0*} = 5$, when the deformation of the droplet is still reversible. Curves 3 (M = 1.07) and 4 (M = 1.8) correspond to supercritical loading $We_{0*} > We_0$. The dashed curve corresponds to the critical deformation stage $\bar{b}_* = 1.7$. The region of validity of the proposed model is bounded by the inequalities $\bar{a} < \bar{a}_*$ and $\bar{b} < \bar{b}_*$.

The calculated $[\bar{b}(t)]$ and measured $[\bar{b}_e(t)]$ [4, 6] dynamics of the deformation of liquid droplets in subcritical loading are compared in Table 1.

Wind tunnel experiments with water droplets (R = 1300 μm) at We_0 = 6.25 are reported in [4], and air shock experiments at M = 1.1 with water droplets (R = 110 μm, We_0 = 3.55) are reported in [6].

In Fig. 2 the calculated function $\bar{b}(\bar{t})$ (solid curve) is compared with experimental data [5] (points) on the deformation of an ethyl alcohol droplet (R = 750 μm) in an air shock with M = 1.56 ($We_0 = 5.6 \cdot 10^3$). This case corresponds to "supercritical" loading of the droplet. According to [5], the abrasion of the droplet by the gas flow begins to accelerate appreciably at $\bar{t} \approx 0.5$, i.e., the droplet begins to lose mass.

Previously [13] it has been found that the time $\bar{t} \approx 0.5$ for a low-viscosity liquid (water) at $We_0 > 5 \cdot 10^2$ corresponds to the onset of shattering of the droplet (R = 400-1700 μm). At $\bar{t} \approx$ 0.5-0.6 the calculated curve in Fig. 2 begins to deviate markedly from the experimental curve (dashed curve), because the mass of the droplet is assumed to be constant in the given model. It is interesting to note that the critical deformation stage of the droplet $\bar{b} \approx \bar{b}_*$ is attained at $\bar{t} \approx 0.5$.

The calculated $\bar{b}(t)$ curve is compared with the experimental data of [15] in Fig. 3. In [15] the deformation of a water droplet (R = 1350 μm) behind air shocks was determined by shadowgraphy at various Mach numbers: M = 1.3 (points 1/curve 6); 1.5 (2/7); 2.0 (3/8); 3.0 (4/9); 3.5 (5/10).

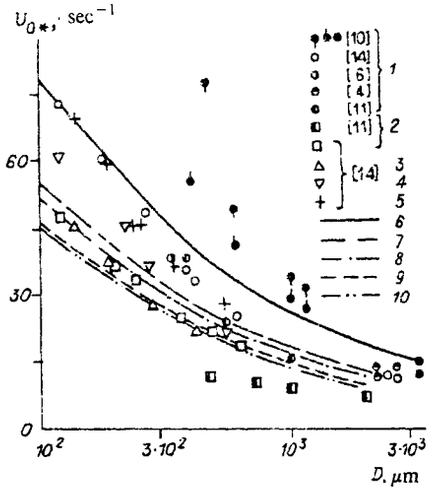

Fig. 4

In all the indicated experiments the loading of the droplet was "supercritical," and the droplets broke up as their surface layer was stripped away by abrasion. Table 2 gives the calculated values of the characteristic time $t_d(M)$ and the time τ at which an appreciable discrepancy begins to be observed between the calculated and experimental results. In Fig. 3 the ratio $\tau/t_d \approx 0.5$, and it does not depend on M. For the indicated values of We_0 (see Table 1) $t \approx 0.5$ corresponds to the onset of abrasion of the droplet surface [13]; this event could account for the discrepancy of the results. As in Fig. 2, we have $\bar{b} \approx \bar{b}_*$ at $\bar{t} \approx 0.5$ for the experimental conditions in [15].

It has been observed experimentally [6] that the dimensionless time of deformation of a droplet in an air shock up to a fixed stage ($\bar{a}$, $\bar{b}$ = idem) is essentially independent of We_0 (in the range $20 < We_0 < 100$ for droplets of silicone oil, R = 100-250 μm). The calculated values of this time for fixed values of $\bar{b}$ and various values of R (We_0) are given in Table 3 for the experimental conditions of [6] ($M = 1.1$). We see that the proposed model agrees satisfactorily with the observations in [6].

The most interesting results pertain to the critical droplet loading regime. Experimental curves of the critical velocity of a steady gas flow U_{0*} as a function of the droplet diameter $D = 2R$ are often published in the literature. In Fig. 4, accordingly, the calculated (curves 6-10) and measured values of the critical velocity of an air flow U_{0*} are compared for droplets of various liquids: water (point 1/curve 6), methyl alcohol (2/7), and oils of various viscosities: 10 St (3/8), 50 St (4/9), and 100 St (5/10).

We note that the experimental data in Fig. 4 have been obtained by different experimental procedures. The breakup of droplets was observed in a free air jet ($\rho = \rho_0$) in [10], in a vertical wind tunnel in [11], and in a shock tube in [14, 4, 6].

It has been noted in certain experiments [4, 10] that a gas velocity transition zone exists, where the droplet is subjected to critical loading. In this regard Fig. 4 shows the lower and upper limits of U_{0*} in the zone. In [10] the lower limit corresponds to simple splitting of the droplet, and the upper value to shattering of the droplet.

It is evident from the comparison of the calculated and experimental data that the proposed model gives satisfactory predictions. It is particularly significant that the model traces the influence of viscosity and surface tension of the liquid.

It follows from Eq. (2.12) that the integral curve in the (We, a) plane is described by the equation

$$\frac{d\overline{We}}{d\bar{a}} = \frac{3}{2}C_x\left(\frac{\overline{We}}{\bar{a}}\right)\left[\left(\frac{\rho}{\rho_l}\right)^{2/3}\left(\frac{\mu_l}{\mu}\right)^{1/3}\right]\left[C_x + (2\bar{a}^3 - \bar{a}^{3/2} - \bar{a}^{-3/2})\right]$$

subject to the initial condition $We = We_0$ at $a = 1$.

Consequently,

$$We_{0*} = f\left(\bar{a}_*, \left[\left(\frac{\rho}{\rho_l}\right)^{2/3}\left(\frac{\mu_l}{\mu}\right)^{1/3}\right]\right),$$

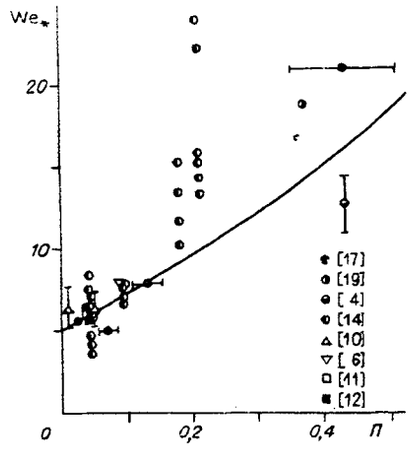

Fig. 5

i.e., for a given $\bar{a}_*$ the critical Weber number depends on a single dimensionless parameter $\Pi = (\rho/\rho_l)^{2/3}(\mu_l/\mu)^{1/3}$. Taking Eq. (3.1) into account, we find that for shock-loaded liquid droplets

$$\mathrm{We}_{0*} = f(\gamma, \mathrm{M}, \left[\left(\frac{\rho_0}{\rho_l}\right)^{2/3}\left(\frac{\mu_l}{\mu_0}\right)^{1/3}\right]).$$

It is interesting to note that the Laplace number is not included in the set of governing parameters for We_{0*}.

Figure 5 shows the calculated $\mathrm{We}_{0*}(\Pi)$ curve. The calculations were carried out for real liquids (mercury, water, alcohol, kerosene, oils, glycerin–water mixtures, pure glycerin, etc.) for $1 < M < 1.2$. In the range $0 < \Pi < 0.5$ the calculated $\mathrm{We}_{0*}(\Pi)$ curve is approximated by the relation

$$\mathrm{We}_*(\Pi) = 5 + 25\Pi + 4\Pi^2.$$

Experimental data [4, 6, 10-12, 14, 17] are shown for comparison. Isshiki's results for glycerin droplets are cited from [4]. The scatter of the data from [17] is attributable to the fact that ranges of variation of R and M and calculated values of La are given in [17] rather than data for specific experiments. The scatter of the results from [4, 10] is associated with the fact that lower and upper bounds of droplet stability are distinguished in the results. The data of [14] stand out among the experimental points in that they exhibit a fairly strong dependence of We_{0*} on the size of the droplets. We have been unable to find experimental data in the ranges $0.2 < \Pi < 0.4$ and $\Pi > 0.45$.

We have thus presented a simple model of the deformation of a liquid droplet in a gas flow. The model is constructed in the preferred direction of deformation approximation and is based on two equations: the droplet deformation equation and its equation of motion. An important parameter governing the droplet deformation rate is the coefficient K, which takes into account the dissipation of energy in the excitation of internal flows of liquid in the droplet. Since $\mu_l >> \mu$ and $\rho_l >> \rho$, the coefficient K is much smaller than unity. All other conditions being equal, the dissipation of energy in the droplet increases with the viscosity of the liquid.

It follows from a comparison of the results of the calculations with experimental data that the model gives satisfactory results for the critical Weber number and the characteristic deformation time of a droplet in the range $0 < \Pi < 0.5$.

REFERENCES

1. A. H. LeFebvre, Gas Turbine Combustion, Hemisphere Publ. Co., Washington, D.C. (1983).
2. W. E. Baker, P. A. Cox, P. S. Westine, et al., Explosion Hazards and Evaluation, Elsevier, Amsterdam (1983).
3. V. M. Boiko, A. N. Papyrin, and S. V. Poplavskii, "Dynamics of the breakup of droplets behind shock waves," Prikl. Mekh. Tekh. Fiz., No. 2 (1987).

4. A. Wierzba, "Deformation and breakup of liquid drops in a gas stream at nearly critical Weber numbers," Exp. Fluids, **9**, 59-64 (1990).
5. T. Yoshida and K. Takayama, "Interaction of liquid droplets with planar shock waves," Trans. ASME J. Fluids Eng., **112**, 423-428 (1990).
6. H. Hirahara and M. Kawahashi, "Experimental investigation of viscous effects upon a breakup of droplets in high-speed air flow," Exp. Fluids, **13**, 231-234 (1992).
7. V. P. Sosnin, I. A. Kopyrin, and S. G. Filimonov, "Mechanism of the deformation and breakup of a mixed droplet," Poroshk. Metall., No. 7, 1-5 (1987).
8. Zheng-Tao Deng and San-Mou Jeng, "Numerical simulation of droplet deformation in convective flows," AIAA Paper No. 90-2369, AIAA, New York (1990).
9. V. S. Surov and V. M. Fomin, "Numerical simulation of the interaction of a water droplet with a strong airborne shock wave," Prikl. Mekh. Tekh. Fiz., No. 1, 48-54 (1993).
10. M. S. Volynskii, "Breakup of droplets in an air flow," Dokl. Akad. Nauk, **62**, 301-304 (1948);, **68**, 237-240 (1949).
11. W. R. Lane, "Shatter of drops in streams of air," Ind. Eng. Chem., **43**, No. 6, 1312-1317 (1950).
12. J. O. Hinze, "Fundamentals of hydrodynamic mechanism of splitting in dispersion process," AIChE J., No. 1, 289-295 (1955).
13. A. A. Buzukov, "Breakup of droplets and jets of liquid by an airborne shock wave," Prikl. Mekh. Tekh. Fiz., No. 2, 154-158 (1963).
14. A. R. Hanson, E. G. Domich, and H. S. Adams, "Shock tube investigation of the breakup of drops by air blasts," Phys. Fluids, **6**, No. 6, 1070-1080 (1963).
15. A. A. Ranger and J. A. Nicholls, "Aerodynamic shattering of droplets," AIAA J., **7**, No. 2, 285-295 (1969).
16. P. G. Simpkins and E. L. Bales, "Water-drop response to sudden accelerations," J. Fluid Mech., **55**, No. 3, 629-639 (1972).
17. B. E. Gel'fand, S. A. Gubin, and S. M. Kogarko, "Characteristics of the breakup of viscous liquid droplets," Inzh.-Fiz. Zh., **25**, No. 3, 467-470 (1973).
18. B. E. Gel'fand, S. A. Gubin, and S. M. Kogarko, "Modifications of the breakup of droplets in shock waves and their characteristics," Inzh.-Fiz. Zh., **27**, No. 1, 119-126 (1974).
19. S. A. Krezeczkowski, "Measurement of liquid droplet disintegration mechanism," Int. J. Multiphase Flow, **6**, 227-239 (1980).
20. A. I. Ivandaev, A. G. Kutushev, and R. I. Nigmatulin, "Gas dynamics of multiphase media: shock and detonation waves in aerocolloids," in: Itogi Nauki Tekh. VINITI Ser. Mekh. Zhidk. Gaza, **16** (1981).
21. A. L. Gonor and N. V. Zolotova, "Slowing and deformation of a liquid droplet in a gas flow," Izv. Akad. Nauk SSSR, Mekh. Zhidk. Gaza, No. 2, 59-69 (1981).
22. G. D. Gordon, "Mechanism and speed of breakup of drops," J. Appl. Phys., **30**, 11-20 (1959).
23. M. S. Volynskii and A. S. Lipatov, "Deformation and breakup of droplets in a gas flow," Inzh.-Fiz. Zh., **18**, No. 5, 838-843 (1970).
24. V. E. Davidson, "Deformation of droplets in a gas flow," in: Jet and Pipe Flows [in Russian], Dnepropetrovsk (1974), pp. 3-35.
25. A. A. Borisov, V. E. Gelfand, S. A. Gubin, et al., "The reaction zone of two-phase detonation," Astronaut. Acta, **45**, 411-417 (1970).
26. S. A. Zhdan, "Simulation of heterogeneous detonation with allowance for deformation and breakup of the fuel droplets," Fiz. Goreniya Vzryva, **13**, No. 2, 258-262 (1977).
27. G. A. Saltanov, Supersonic Two-Phase Flows [in Russian], Vysshaya Shkola, Minsk (1972).
28. M. E. Deich, Engineering Gas Dynamics [in Russian], Gosénergoizdat, Moscow (1961).
29. R. C. Reid, J. M. Prousnitz, and T. K. Sherwood, The Properties of Gases and Liquids, McGraw-Hill, New York (1980).